Estimating Polarization Purity With Noise

Alexander Kostinski[©], Daniel Kestner[©], and Jothiram Vivekanandan

Abstract—We formulate a problem of estimating and monitoring mismatch (unwanted departure from orthogonality) of two ostensibly orthogonal polarization channels in a fully polarimetric general device such as a polarimetric weather radar. A statistical approach is proposed by using thermal noise or, more generally, a "polarimetric noise" class of sources. The suitable noise class of distributions is shown to be rooted in the complex multivariate Gaussian probability density function (pdf), the latter possessing a uniform pdf on the Poincare sphere (PS), with a probability measure given by a fractional surface area. To that end, we develop a parameter to estimate polarization purity. By relating an inner (dot) product of noisy electric fields to their cross-correlation coefficient, we arrive at a simple relation between the ellipticity δ_{ϵ} and tilt δ_{τ} mismatches and the measured complex voltage cross-correlation coefficient ρ : $\rho \approx \mp \cos(2\epsilon)\delta_{\tau} \pm i\delta_{\epsilon}$. Our results are confirmed by Monte Carlo simulations. Thermal noise microwave data collected by the S-band radar of the National Center for Atmospheric Research (NCAR) during solar calibration scans is used to set bounds on δ_{ϵ} and δ_{τ} , thereby characterizing polarization purity.

Index Terms-Imbalance, noise, polarimetry, radar.

I. INTRODUCTION

PHASED array configuration is currently being considered as a leading contender for next-generation weather radars in the USA. The polarization diversity is an important of part of the design and the change in transmitted polarization will be accomplished digitally, along with the beam steering. This renders precise timing a particularly important requirement for avoiding phase errors in the arrays [1]. Timing errors can turn into polarization errors (ellipticity, in particular), and here, we shall focus on polarimetry within the context of distributed weather targets. The state of polarization typically changes as the weather radar beam is steered away from broadside [2] and such changes have been thoroughly modeled by others by assuming the cross-dipole configuration and other specific architectures [3], [4].

The question we pose and address here complements these modeling studies as our goal is not to predict polarization errors but rather to detect and estimate them. Throughout

Manuscript received 22 January 2024; revised 7 March 2024; accepted 13 March 2024. Date of publication 21 March 2024; date of current version 4 April 2024. This work was supported in part by the National Center for Atmospheric Research (NCAR), which is a major facility sponsored by the U.S. National Science Foundation (NSF) under Agreement 1852977, in part by NSF/NCAR under Agreement AGS-1755088, in part by the National Oceanic and Atmospheric Administration (NOAA) under Award NA18OAR4590431, and in part by NSF under Grant AGS-2217182. (Corresponding author: Alexander Kostinski.)

Alexander Kostinski and Daniel Kestner are with the Department of Physics, Michigan Technological University, Houghton, MI 49931 USA (e-mail: kostinsk@mtu.edu).

Jothiram Vivekanandan is with the National Center for Atmospheric Research, Boulder, CO 80301 USA.

Digital Object Identifier 10.1109/TGRS.2024.3380531

this article, by polarimetric errors or mismatches, we mean a departure from perfect orthogonality of two (ostensibly orthogonal) polarization channels. We shall try here to accomplish the task of estimating these mismatches in a parsimonious, model-independent manner. It may become important to monitor polarization purity in real time, e.g., during weather radar observations and then distributed targets themselves may serve as a source for polarimetric calibration.

To motivate the basic problem, recall that one must measure the ellipticity and tilt of the instantaneous polarization ellipse of incident (and/or transmitted) electromagnetic radiation accurately enough to clearly separate system-inherent polarization errors from polarization changes caused by the distributed targets. But to do that, one needs to know, to what precision the two orthogonal channels of a polarimteric radar basis are actually orthogonal. It is particularly desirable to have such capability while the weather radar system is in operation. This is the problem considered here, and our goal is to devise a method with minimal assumptions regarding modeling of the propagation media.

To that end, here we propose a method for detecting polarization nonorthogonality in a pair of ostensibly cross-polarized receivers via a "noisy," or unpolarized input. This method is suggested by an analogy with detecting phase error in quadrature receivers, previously implemented in [5], [6], and [7]. That method was developed to employ weather radar signals from precipitation, the latter stochastic because of the hydrometeors' random location and size distribution. The real (I) and imaginary (Q) components of the received weather signals are zero mean, statistically independent and identically distributed (IID) Gaussian random variables [8], [9]. Simultaneous quadrature signals I and Q are statistically independent and have the same autocorrelation function (ACF).

In a dual-polarized radar, the co- and cross-polarized simultaneous I and Q values are also statistically independent, although not necessarily identically distributed because of differential reflectivity. Whatever the target is, however, it must always be required that the polarization states of the dual-channel receivers are orthogonal so that the transmitted signal has negligible cross-polarization contamination. Such orthogonality in radar measurements is essential to secure unbiased estimates of dual-polarimetric observations. This requirement is likely to become more stringent for the next-generation phase array implementation of polarimetric radars.

By a way of motivation, consider the slant $\pm 45^{\circ}$ design of transmitting horizontally (H) and vertically (V) polarized waves, currently being examined at the National Center for Atmospheric Research (NCAR) and one with a long history, see [10]. Right from the outset it requires a π phase shift to

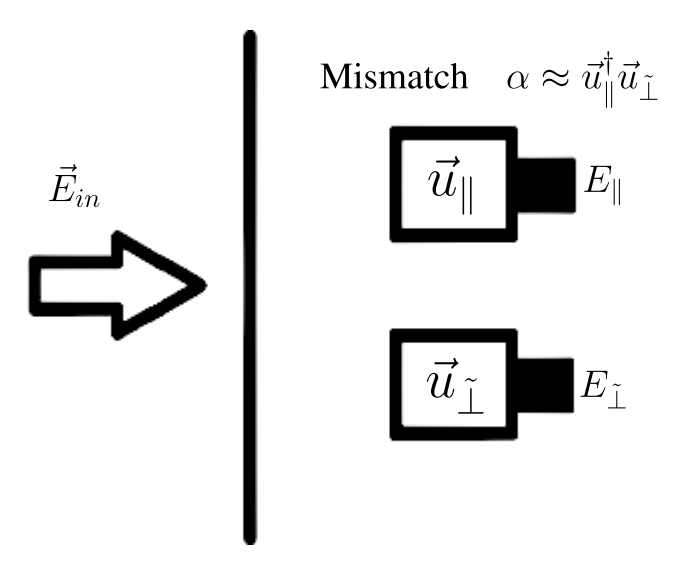


Fig. 1. Sketch of the detection problem. Two (nearly) orthogonal receivers, denoted by hollow rectangles, resolve incident radiation $\vec{E}_{\rm in}$ field into two components: polarization states represented by complex unit vectors \vec{u}_{\parallel} and \vec{u}_{\perp} (e.g., horizontal and (near) vertical, H and V of a linear basis, and left-handed polarization (LCP) and right-handed polarization (RCP) of the circular basis). Measured amplitude $(E_{\parallel}, E_{\perp})$ outputs (voltages) are depicted with filled rectangles. The tilde in the subscript above \perp indicates the deviation from perfect orthogonality, quantified by the generally complex quantity α . The question we pose is: how to estimate the orthogonality mismatch α from measurements of complex amplitudes (proportional to voltages) E_{\parallel} and E_{\perp} .

get from the $\pm 45^{\circ}$ hardware to the HV orthogonal basis. But how does one ensure that the phase shift is exactly 180° rather than, say, 179° ? This type of question led us to the research reported here and, insofar as phased arrays are all about phase shifts, this is an important question to consider.

Polarimetric weather radar systems are typically calibrated using one of the following: sphere calibration, radar observations of precipitation, and solar calibration [4], [9], [11]. Sphere calibration and backscatter from precipitation are used for calibrating transmitter and receiver subsystems. Randomly polarized solar microwave radiation is often used to calibrate dual-channel receivers, and this is our main interest here. Specifically, we shall focus on the deviation from orthogonality and, for the sake of clarity, shall use receiver calibration as a practical example.

II. MATHEMATICAL FRAMEWORK

A typical polarimetric radar setup (in the receiving mode) is sketched in Fig. 1, where a stochastic incident electric field $\vec{E}_{\rm in}$ irradiates two (presumably) orthogonal channels. In order to focus on the state of polarization, separately from the absolute calibration of intensity, we shall denote polarization states by \vec{u} (u for unitary or unit magnitude). Such normalized 2-D complex vectors (variously called polarization states, Jones vector or spinors [12], [13], [14]) are typically represented as $\vec{u} = [\cos(\beta), \sin(\beta)e^{i\phi}]^{\rm T}$, with the superscript T denoting transpose. This representation holds in any basis but if we define β and ϕ in the HV basis; then, H and V are represented as $\vec{u} = [1,0]^{\rm T}$ and $\vec{u} = [0,1]^{\rm T}$, respectively, whereas the angle β defines the electric field tilt for a linearly polarized wave, e.g., $\vec{u} = 1/(2)^{1/2}[1,1]^{\rm T} = [\cos(45^{\circ}), \sin(45^{\circ})]^{\rm T}$. The circular right and left polarizations in the same HV basis are

represented as $\vec{u} = 1/(2)^{1/2}[1, j]^{T}$ and $\vec{u} = 1/(2)^{1/2}[1, -j]^{T}$, respectively [15].

Returning to the general basis setup of Fig. 1 (e.g., circular right and left bases), the incoming radiation is resolved by the two receiver channels into two components \vec{u}_{\parallel} and \vec{u}_{\perp} . The tilde in the subscript above \perp indicates that the (Hermitian) orthogonality is neither perfect either because of the geometric arrangement or phase difference or nor is perfect. The problem posed here is to estimate and monitor these departures from exact orthogonality between the two ostensibly orthogonal channels. Note that the absolute magnitude calibration is neither considered nor do we invoke any models of the scattering medium (unlike [9], [11], and [16], where the notion of a scattering matrix is employed from the outset).

A key step is to find the simplest route to capture the (complex) mismatch mathematically. To that end, we represent the deviation from orthogonality by writing the Jones vector of the near orthogonal antenna (\vec{u}_{\perp}) as a sum of the true orthogonal vector (\vec{u}_{\perp}) and a small projection onto the parallel channel Jones vector (\vec{u}_{\parallel}) due to the nonorthogonality (mismatch). Thus, we can write

$$\vec{u}_{\tilde{\perp}} \equiv \frac{\vec{u}_{\perp} + \alpha \vec{u}_{\parallel}}{\left(1 + |\alpha|^2\right)^{\frac{1}{2}}}.\tag{1}$$

Returning to the polarization mismatch (departure from exact Hermitian orthogonality $\vec{u}_{\perp}^{\dagger}\vec{u}_{\parallel}=0$), the latter is captured by the complex variable α , which is implicitly defined by (1). The Hermitian conjugate symbol \dagger denotes the conjugate transpose, and conjugation has the meaning of reversing the sense of rotation for a polarization ellipse. Although we introduce α with a small deviation in mind ($|\alpha| \ll 1$), \vec{u}_{\parallel} and \vec{u}_{\perp} are left generic in (1) so that α ranges in magnitude from 0 (perfectly orthogonal channels, $\vec{u}_{\perp} = \vec{u}_{\perp}$), to ∞ (parallel channels, $\vec{u}_{\perp} = \vec{u}_{\parallel}$).

The mismatch α can also be expressed explicitly in terms of \vec{u}_{\parallel} and $\vec{u}_{\tilde{\perp}}$, by taking the inner product of both sides of (1) with each of these antenna polarizations, in turn, and combining the results

$$\alpha = \frac{\vec{u}_{\parallel}^{\dagger} \vec{u}_{\perp}}{\vec{u}_{\perp}^{\dagger} \vec{u}_{\perp}}.$$
 (2)

This mismatch expression, reminiscent of a crosstalk, together with (1) yields, to 1st order in ($|\alpha| \ll 1$)

$$\alpha \approx \vec{u}_{\parallel}^{\dagger} \vec{u}_{\tilde{\perp}} \tag{3}$$

as is also indicated by the legend of Fig. 1. Thus, α encapsulates and quantifies our approach to polarization purity.

Randomness enters the development now as our next move is to relate this a priori unknown complex mismatch α to the measured received electric field (complex voltage) *cross correlation coefficient*. Why the cross correlation to estimate α ? We were guided by the fact that both α and the Pearson cross-correlation coefficient ρ at zero lag are the inner products. The latter can be viewed as a cosine of an angle between two random variables, regarded as elements of a functional space [17] but it will be shown here to be related to actual angles, describing mismatches in ellipticity and tilt.

However, for the cross-correlation idea to work, the incident field has to be "sufficiently random" as a simple counterexample suffices to show. Indeed, consider a 45° linearly polarized incident wave, decomposed by an HV dual-polarized receiver. Although the two channels are perfectly orthogonal, the correlation coefficient between them is unity. This is contrary to a perfectly random incident polarization (e.g., precipitation returns from a vertically pointing radar, solar microwave emission, or thermal noise), where one intuitively expects zero correlation between the H and V channels, see [11], which brings us to Section III.

III. RELATING MISMATCH TO COMPLEX CROSS-CORRELATION COEFFICIENT FOR RANDOM INCIDENT POLARIZATIONS

For an incident electric field E (measured complex voltage), the Pearson cross-correlation coefficient between any two channels is given by

$$\rho(E_1, E_2) \equiv \left\langle \frac{E_1 - \langle E_1 \rangle}{\sigma_{E_1}} \left(\frac{E_2 - \langle E_2 \rangle}{\sigma_{E_2}} \right)^* \right\rangle \tag{4}$$

yielding for zero-mean fields

$$\rho(E_1, E_2) = \frac{\left\langle E_1 E_2^* \right\rangle}{\sigma_{E_1} \sigma_{E_2}} \tag{5}$$

where the averaging over a random ensemble is implied by the angular brackets, i.e., for random variables x and y, $\langle xy \rangle \equiv \int xyp(x,y)dxdy$ with p(x,y) being the joint pdf and σs are the associated standard deviations.

The statistics of the randomly polarized incident radiation, such as sun microwave emission or thermal noise, are those of the multivariate circular Gaussian pdf [8], [18]. The joint pdf can be expressed in terms of the four in-phase and quadrature IID components (two for each polarization) or, more generally, in four real variables E_x' , E_x'' , E_y' , and E_y'' with $E_x = E_x' + i E_x''$, $E_y = E_y' + i E_y''$, as $p(E_x', E_x'', E_y', E_y'')$

$$p(E_x', E_x'', E_y', E_y'') = \left(\frac{1}{2\pi\sigma^2}\right)^2 e^{-\frac{E_x'^2 + E_x''^2 + E_y''^2 + E_y''^2}{2\sigma^2}}.$$
 (6)

The model is called circular because the variances of real and imaginary parts are equal for a given direction [8]. Hence the name "multivariate circular Gaussian model" (MCGM). The MCGM pdf is almost invariably derived in the radar meteorology literature by an appeal to the central limit theorem (CLT) [9], [18], e.g., when justifying MCGM for precipitation backscatter. But CLT arguments work well near the center of the pdf but not in the far tails. There is another and exact route to MCGM pdf of (6). The pdf can be deduced from two requirements only: 1) isotropy (rotational invariance) in the space of four random variables and 2) statistical independence [17]. In the context of polarimetry, the MCGM pdf maps onto a uniform pdf of polarization ellipses on the Poincare sphere (PS) as discussed below.

Now observe that (4) is general but when the channels are exactly orthogonal and the observed radiation is sufficiently random, the cross correlation vanishes: $\rho = 0$. The meaning of "sufficiently random" is discussed below but the joint pdf of MCGM in (6) fits the bill. Loosely, any unpolarized and noise-like radiation, e.g., backscatter from precipitation, suffices.

Thus, the main idea of this article is that the deviation from orthogonality causes deviation from $\rho = 0$ as proven below and this suggests that various mismatches between imperfectly orthogonal channels can be *quantified* by observing simple thermal noise. This notion was used for in-phase and quadrature monitoring in the radar and nuclear magnetic resonance (NMR) receiver contexts [5], [6], [7], and a similar idea was employed to explore differential phase versus the fluctuating state of polarization in [19]. Here, we posit a polarimetric analog, likely to be particularly useful in the context of polarimetric phased array weather radar [4], [20], [21], [22].

The polarimetric mismatch problem is solved below at the confluence of three lines of reasoning. First, we argue that perfect (for our purposes) polarimetric noise is the circular Gaussian (IID) process whose density on the PS is uniform, that is, $pdf = dA/4\pi$, with the spherical surface area element $dA = \sin(\theta)d\theta d\phi$. The marginal pdfs are: $f(\phi) = 1/2\pi$ and $f(\theta) = \sin(\theta)/2$. In our Monte-Carlo simulations, the complex field circular Gaussian process (MCGM) [9], [23] indeed yields the uniformity. Second, we treat probability as a measure, i.e., the probability of a polarization state within a given tolerance equals the corresponding (fractional) area on the spherical PS surface. Third, the Jones vector formalism and a small parameter expansion are employed to arrive at a simple relationship between polarization imbalance and the cross-correlation coefficient.

Let us now address the last item and consider the field cross-correlation coefficient between two nearly orthogonal polarization channels, denoted by $\rho_{\parallel \tilde{\perp}}$. Specializing the definition of cross correlation coefficient (4) to the case at hand, we get

$$\rho_{\parallel\tilde{\perp}} \equiv \frac{\left\langle E_{\parallel} E_{\tilde{\perp}}^* \right\rangle}{\sigma_{\parallel} \sigma_{\tilde{1}}} \tag{7}$$

where σs are the corresponding standard deviations and $\sigma_{\parallel} = \sigma_{\tilde{\perp}}$ is assumed. Throughout the rest of this article, we drop the subscripts in $\rho_{\parallel \tilde{\perp}}$ and use a simple ρ instead, except in the S-Pol radar section, where ρ_{HV} is used. Note that this ρ_{HV} is distinct from the traditional ρ_{HV} of weather radar polarimetry. The latter is a measure of the similarity of co-polar HH and VV returns and is typically near unity whereas ours is typically near 0 and measures deviation from the polarization orthogonality.

As above, the statistical average is denoted by angular brackets $\langle \rangle$, and it is an integral of the variable in question [such as E_{\parallel} in (7)] over the space spanned by the complex fields E_x and E_y , and weighted by their joint pdf $p(E_x, E_y)$.

In order to relate α to the field cross-correlation coefficient ρ , we first work toward the numerator of ρ in (5)

$$E_{\parallel} = \vec{u}_{\parallel}^{\dagger} \vec{E}_{\text{in}}; \quad E_{\perp} = \vec{u}_{\perp}^{\dagger} \vec{E}_{\text{in}}$$
(8)

$$E_{\perp} = \left(\frac{\vec{u}_{\perp} + \alpha \vec{u}_{\parallel}}{(1 + |\alpha|^{2})^{\frac{1}{2}}}\right)^{\dagger} \vec{E}_{\text{in}}$$

$$= \frac{1}{(1 + |\alpha|^{2})^{\frac{1}{2}}} \left(\vec{u}_{\perp}^{\dagger} \vec{E}_{\text{in}} + \alpha^{*} \vec{u}_{\parallel}^{\dagger} \vec{E}_{\text{in}}\right)$$

$$= \frac{1}{(1 + |\alpha|^{2})^{\frac{1}{2}}} (E_{\perp} + \alpha^{*} E_{\parallel})$$
(9)

and the numerator in (7) becomes

$$\left\langle E_{\parallel} E_{\perp}^{*} \right\rangle = \frac{1}{\left(1 + |\alpha|^{2}\right)^{\frac{1}{2}}} \left(\left\langle E_{\parallel} E_{\perp}^{*} \right\rangle + \alpha \left\langle |E_{\parallel}|^{2} \right\rangle \right). \tag{10}$$

We digress briefly to interpret the above equations and recall that the complex voltage measured by a dual-polarized antenna in polarization state \vec{u}_1 in response to the incident field of polarization \vec{u}_2 is proportional to the Hermitian product $\vec{u}_1^{\dagger} \vec{u}_2$ († denoting the conjugate transpose). The conjugation of the Hermitian transpose † reverses the sense of rotation of the polarization ellipse, described by $\vec{u} = [\cos(\beta), \sin(\beta)e^{i\phi}]^{T}$. By reciprocity, the antenna polarization in transmitting and receiving modes (so-called antenna height, [24], [25]) are related by conjugation. The resultant helicity thus depends on the context [12] and does not affect the present formalism. For example, a dual-polarized receiver with the circular right and left polarized basis, given in the HV system by $\vec{u}_1 = 1/(2)^{1/2}(1, j)$ and $\vec{u}_2 = 1/(2)^{1/2}(1, -j)$ with their inner product being 0. Also, the inner product of an antenna in polarization $\vec{u}_1 = 1/(2)^{1/2}(1, j)$ and incident wave with polarization $\vec{u}_2 = 1/(2)^{1/2}(1, -j)$ is given by $(1/2)(1, j)^{\dagger}(1, -j) = 1 + j^2 = 0$ as it should.

Returning to the main derivation and to advance further toward a simple expression, we use statistical independence of the zero-mean fields E_{\parallel} and E_{\perp} so that only the second term survives the averaging $\langle \rangle$ in the above expression. We can thus obtain

$$\left\langle E_{\parallel} E_{\perp}^{*} \right\rangle = \frac{\alpha}{\left(1 + |\alpha|^{2}\right)^{\frac{1}{2}}} \left\langle |E_{\parallel}|^{2} \right\rangle. \tag{11}$$

With equal variance in addition to the independence assumption, (explicitly satisfied by the classical joint circular Gaussian pdf on natural unpolarized radiation, see [8] but also [26])

$$\sigma_{\parallel}^2 = \sigma_{\tilde{1}}^2 = \left\langle |E_{\parallel}|^2 \right\rangle \tag{12}$$

finally yielding for the cross correlation coefficient

$$\rho = \frac{\alpha}{\left(1 + |\alpha|^2\right)^{\frac{1}{2}}}.\tag{13}$$

For small mismatches, we arrive at the remarkably simple expression for the unknown mismatch in terms of measured (sample) cross-correlation coefficient.

$$\alpha \approx \rho$$
. (14)

This in itself, apart from applications, is already an important theoretical result. Here, we press on to express this equation in explicitly terms of ϵ and τ , as defined in Fig. 2. We remark that for the more general case of unequal received intensity variances (e.g., joint "elliptical" Gaussians), the cross-correlation corresponding to incident fields that are independent in the orthogonal \vec{u}_\parallel \vec{u}_\perp basis, generalizes to

$$\rho = \left(\frac{\sigma_{\parallel}}{\sigma_{\tilde{\perp}}}\right) \frac{\alpha}{\left(1 + |\alpha|^2\right)^{\frac{1}{2}}}.$$
 (15)

The prefactor $(\sigma_{\parallel}/\sigma_{\perp})$ is essentially a square root of differential reflectivity (Z_{DR}) when the radar basis is HV. Thus, if Z_{DR} is measured at the same time, (15) permits nonorthogonality estimation during actual weather observations.

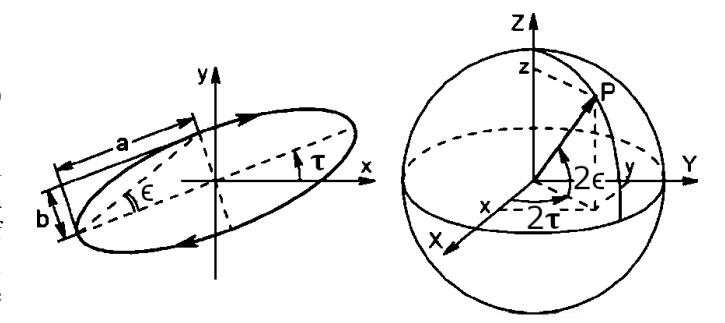


Fig. 2. (Left) Polarization ellipse and (right) its representation on the PS. Ellipticity is characterized by the axial ratio (b/a), 0 < b < a, and the ellipticity angle $\epsilon = \pm \tan^{-1}[(b/a)]$, positive for RCPs, a clockwise rotation looking into the beam (see [13], p. 28), and negative for LCP, ranging from $-\pi/4$ to $\pi/4$ (from LCP to RCP), $\epsilon = 0$ (equator) for the linear ones. The angle of the major axis w.r.t +x-axis is the tilt angle τ , ranging from $-\pi/2$ to $\pi/2$, consistent with the range of inverse tangent [27]. The associated PS angles (position P) are 2ϵ and 2τ , ranging from $-\pi/2$ to $\pi/2$ and $-\pi$ to π , respectively.

IV. MISMATCHES ON THE POINCARE SPHERE

We now proceed to express the results directly in terms of ellipticity ϵ and tilt τ of the polarization ellipse, see Fig. 2, to render setting tolerances on measurements of, say, radar differential reflectivity, Z_{DR} or differential phase, K_{DP} more intuitive. In this emphasis on ϵ and τ , we follow [11] who were first to examine polarimetric weather radar performance specifically in terms of ellipticity and tilt but we choose the PS device to express mismatch α , a complex variable, in terms of ϵ and τ . By employing the sphere, we take advantage of the joint circular Gaussian pdf mapping onto a uniform pdf on the spherical surface. Then, the probability of having a polarization ϵ_0 and τ_o within some tolerances is simply the fractional area on the sphere (probability as a measure). To recap so far, taking the scalar product of (1) led us to expression for mismatch in terms of the Jones vector inner product

$$\vec{u}_{\parallel}^{\dagger} \vec{u}_{\perp} = \frac{\alpha}{\left(1 + |\alpha|^2\right)^{\frac{1}{2}}} \tag{16}$$

but with the Jones vectors now viewed as functions of ellipticity and tilt.

Equation (13) for the cross-correlation coefficient, using (16) can be written simply and generally in terms of the inner product of antenna Jones vectors

$$\rho = \vec{u}_{\parallel}^{\dagger} \vec{u}_{\tilde{\perp}}. \tag{17}$$

We shall denote the ellipticities and tilts of our basis $a\vec{u}_{\perp}$ and \vec{u}_{\parallel} as ϵ_{\perp} , ϵ_{\parallel} and τ_{\perp} τ_{\parallel} , respectively. Perfectly orthogonal polarization ellipses are antipodal, lying on opposite sides of the PS. In terms of their ellipticity and tilt, $\epsilon_{\perp} = -\epsilon_{\parallel}$, and $\tau_{\perp} = \tau_{\parallel} \pm (\pi/2)$. The sign of $(\pi/2)$ is such that the tilt is kept in the range $-(\pi/2)$ to $(\pi/2)$.

Returning to (17), it can be shown that the magnitude of $\rho = |\rho|e^{i\phi}$ is $|\rho| = \cos(\theta/2)$, where the angle θ is also the arc length between \vec{u}_{\parallel} and \vec{u}_{\perp} on the (unit radius) sphere (Fig. 2) [28]. Orthogonal states are antipodal (on opposite sides of the PS), so it is convenient to work with the deviation from

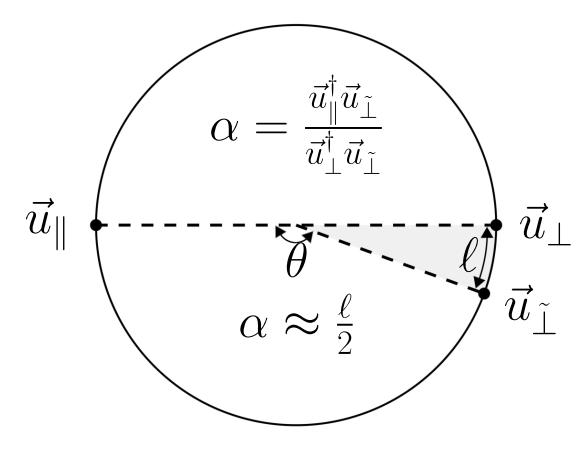


Fig. 3. Link from the mismatch α to the instrumental tolerances δ_{ϵ} and δ_{τ} , provided by the PS. For any polarization state \vec{u}_{\parallel} , its orthogonal polarization, \vec{u}_{\perp} is the antipodal point on the PS (cross section shown). Polarization states, \vec{u}_{\perp} , nearly orthogonal to \vec{u}_{\parallel} lie a small "mismatch are length" (shaded sector), away. Are length is the geodesic distance between \vec{u}_{\perp} and \vec{u}_{\perp} , i.e., from $(2\epsilon, 2\tau)$ to $(2\epsilon + 2\delta_{\epsilon}, 2\tau + 2\delta_{\tau})$. The polarization mismatch α is related to the arc length l as $l = 2 \tan^{-1}(|\alpha|) \approx 2\alpha$.

antipodality and write $l = \pi - \theta$. Then, $|\rho| = \sin((l/2)) \approx (l/2)$, where l is the arc length between \vec{u}_{\perp} and \vec{u}_{\uparrow} (Fig. 3).

We shall denote the ellipticity and tilt deviations from the orthogonality of the (presumably) perpendicular state $u_{\tilde{\perp}}$ as δ_{ϵ} and δ_{τ} , respectively. For small l, according to Pythagoras' theorem in the planar approximation, $l=((2\delta_{\epsilon})^2+(2\cos(2\epsilon)\delta_{\tau})^2)^{1/2}$. This leads to the following expression for the magnitude of ρ in terms of ellipticity and tilt errors: $|\rho|=(l/2)=(\delta_{\epsilon}^2+\cos^2(2\epsilon)\delta_{\tau}^2)^{1/2}$. This indicates how cross correlation arises from independent tilt error and ellipticity error, for incident polarized fields with a uniform density on the sphere. For such fields, the field intensity coefficient ρ_I is a square of the complex cross-correlation magnitude: $\rho_I=|\rho|^2$. Taking a square root (see [28] for details) in the small error approximation, to 1st order, then yields

$$\rho = \vec{u}_{\parallel}^{\dagger} \vec{u}_{\tilde{\perp}} \approx \mp \cos(2\epsilon_{\parallel}) \delta_{\tau} \pm i \delta_{\epsilon} \tag{18}$$

where the upper sign is for τ_{\parallel} in the 4th quadrant, and the lower sign for τ_{\parallel} in the 1st quadrant. Given the smallness of the δs in this work, the \pm for various quadrants can be omitted in practice. Equation (18) can also be verified as a small angle expansion of an exact result, derived recently in a physics context [28], [29]. This is a completely general result for the inner (scalar) product of two polarization states u_1 and u_2 : $u_1^{\dagger}u_2 = \cos(\tau_2 - \tau_1)\cos(\epsilon_2 - \epsilon_1) + i\sin(\tau_2 - \tau_1)\sin(\epsilon_2 + \epsilon_1)$.

In the present context, however, it is the approximate (18) that encapsulates our main result and, to leading order, elegantly decouples ellipticity and tilt contributions: with ellipticity being solely responsible for the imaginary part. In this regard, we note that modeling studies of specific radar systems, in contrast to the present work, assumed orthogonality of tilt and ellipticity errors (see [11, eq. (8)]) and the ellipticity error was found to dominate the total error.

Although our mathematical framework is developed with the view of a completely general polarimetric basis, special cases of practical interest in current weather radars are the HV and circular bases: 1) pure linear polarization; $\rho \approx \mp \delta_{\tau}$ and

2) purely circular polarization; $\rho \approx \pm i \delta_{\epsilon}$, with the linear/circular duality of the answers. For the circular basis, where \parallel is RCP, $\rho = \delta_{\epsilon}$ while for the horizontal/vertical basis, $\parallel = H, \, \rho = \delta_{\tau}$, assuming, for the sake of clarity, that $\tilde{\perp}$ is not contaminated by an ellipticity error. Both cases are confirmed via simulation as shown in Fig. 4 and detailed next.

V. MONTE CARLO CONFIRMATION

To test (18) for polarimetric noise observations, we simulated the joint circular Gaussian pdf model for incident radiation, see [8]. This distribution is the "gold standard" for modeling distributed targets and yields a uniform pdf of polarization states on the PS, see [30]. We used the built-in MATLAB function (randn, 1i option) to generate complex number samples of zero-mean unit variance circular normal $\mathcal{CN}(0, 1)$. This corresponds to the real and imaginary parts having variance (1/2). Incident radiation intensities satisfy $\langle |E_x|^2 \rangle = \langle |E_y|^2 \rangle = \langle I_{\parallel} \rangle = \langle I_{\perp} \rangle = 1/2$ with an associated uniform pdf on the unit sphere. We then calculated the measured fields (complex voltages) as $E_{\parallel} = \vec{u}_{\parallel}^{\dagger} \vec{E}_{\rm in}$ and $E_{\perp} = \vec{u}_{\perp}^{\dagger} \vec{E}_{\rm in}$. In passing, we note that this method of generating uniform distributions via simulation of multivariate Gaussians is often employed in statistics on spheres [31].

For each pair of the mismatches, δ_{ϵ} and δ_{τ} , we generated 10^4 independent samples of Jones vectors $\vec{u}_{\rm in}$ from the circular multivariate Gaussian ensemble $\mathcal{CN}(0,1) \times \mathcal{CN}(0,1)$ and, with the given \vec{u}_{\parallel} and \vec{u}_{\perp} , calculated the associated E_{\parallel} and E_{\perp} . We then calculated the cross-correlation coefficient ρ for this ensemble of 2×10^4 values for each data point, to generate the two panels of Fig. 4. In passing, we note that the procedure can generate univariate Gaussian with a specified Doppler spectrum as well (e.g., so that the pulse pair techniques can recover the spectrum).

The bottom x-axis in both panels are in radians to illustrate the slope of ± 1 predicted by (18), represented by the solid lines, and the top x-axis is shown in degrees for practical convenience.

Recall that the sample cross correlation coefficient is a (fluctuating) random variable and is, therefore, associated with some statistical uncertainty, even for large sample sizes. In passing, we note that in the statistical signal processing literature, the common notation for the *sample* cross-correlation coefficient would be $\hat{\rho}$ rather than ρ but there is no ambiguity in the current context.

VI. THERMAL NOISE FROM SOLAR SCAN DATA COLLECTED BY NCAR S-POL-RADAR

To apply (18) in the weather radar context, we examined data from NCAR S-Pol's radar system [32]. S-Pol has a horizontal/vertical basis and, therefore, $\cos(2\epsilon_{\parallel})=1$ and (18) reduces to

$$\delta_{\tau} + i\delta_{\epsilon} = \text{Re}(\rho_{\text{HV}}) + i\text{Im}(\rho_{\text{HV}})$$
 (19)

where the right-hand side (RHS) is calculated from measured data, thereby establishing bounds on the two polarization mismatches on the left-hand side (LHS) of (19).

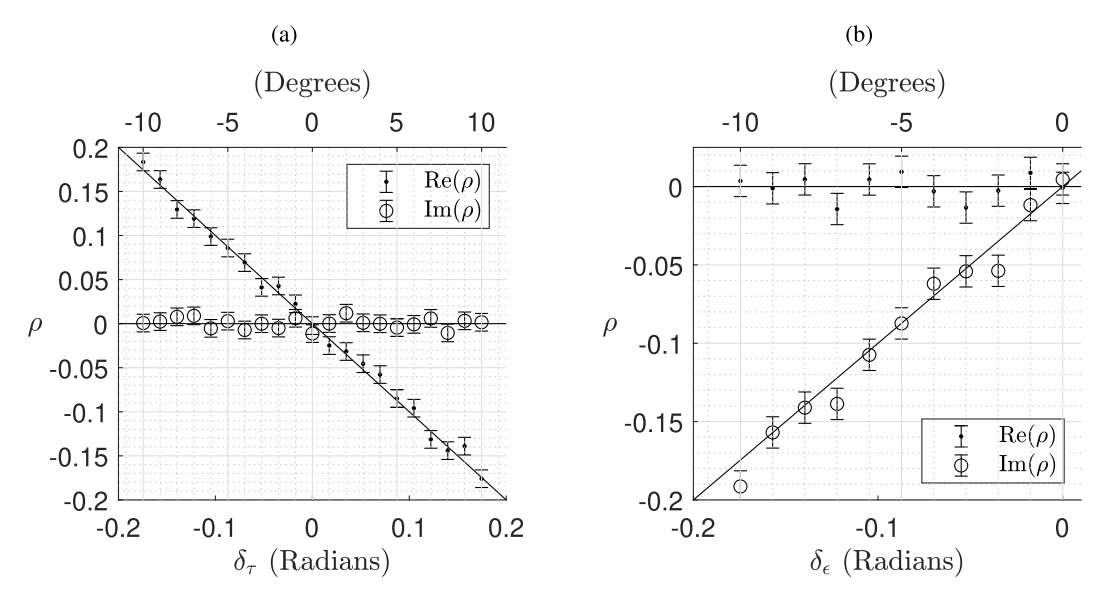


Fig. 4. Monte Carlo confirmation of theoretical results. (a) Sample (complex) cross-correlation coefficient ρ versus tilt imbalance δ_{τ} for (nearly) $\pm 45^{\circ}$ linear receivers. The -45° antenna is held fixed, while the other receive antenna ranges from $+35^{\circ}$ to $+55^{\circ}$ in 1° increments. The real part fits well to a linear dependence with slope -1 and no offset, which is shown by the solid line, as predicted in (18). The vertical error bars display the $1/(N)^{1/2} = 10^{-2}$ range of uncertainty in the computed cross-correlation coefficient for the sample size $N = 10^4$. The imaginary part is approximately 0 and does not depend on the tilt error, in agreement with (18). (b) Right and left circular polarization antennae of the receiver form the basis for polarization measurements here. The right circular antenna departs from $\epsilon = +\pi/4$ by a given δ_{ϵ} on the x-axis. Error bars on ρ are as in (a). The real part of ρ does not depend on the ellipticity error, and its imaginary part shows a linear dependence in the error, both in agreement with (18).

We used time-series data from the S-Pol radar (NCAR/EOL S-Pol Team, 2023) collected in 2002 during the PRECIP field campaign in Taiwan. [33] The S-Pol time-series data is available at https://doi.org/10.26023/EMAT-JPBX-S20T (NCAR/EOL S-Pol Team, 2023). The time-series data were converted from their original TsArchive format to NetCDF using the Ts2NetCDF utility from the Lidar Radar Open Software Environment (LROSE, http://lrose.net/).

We selected solar scan receiver calibration time series as illustrated by range gate 1500 in Fig. 5. Although the range gates have no particular significance during such solar scans designed to calibrate the receiver, the transmitter was kept on at full power, in order to ensure S-Pol's circuitry's proper operating temperature (John Hubbert, personal communication). The data for near-range gates, corresponding to smaller gate numbers, contained ground clutter (ground reflection by sidelobes) and, therefore, range gates below 400 were avoided in our analysis.

We examined the raw data of digital counts (from an A/D converter), consisting of scalar time-series of voltage at each antenna polarization, measured for in-phase (I) and quadrature (Q) components, for each of the H and V polarizations. This data quartet of panels in Fig. 5 is arranged as in-phase and quadrature data for the horizontally and vertically polarized channels of the dual-polarized S-Pol's receiver. This particular data segment represents an azimuth scan across the solar disk at a fixed elevation angle of 20.7° and spans about 7° in azimuth. These solar scan data were recorded on June 23, 2022 at 22:51:53 UTC.

Although solar microwave emission is an ideal example of jointly normal circular Gaussian pdf, it is not stationary as the scan data of Fig. 5 has a hump in the middle portion, corresponding to the radar beam (0.92°) being centered on the

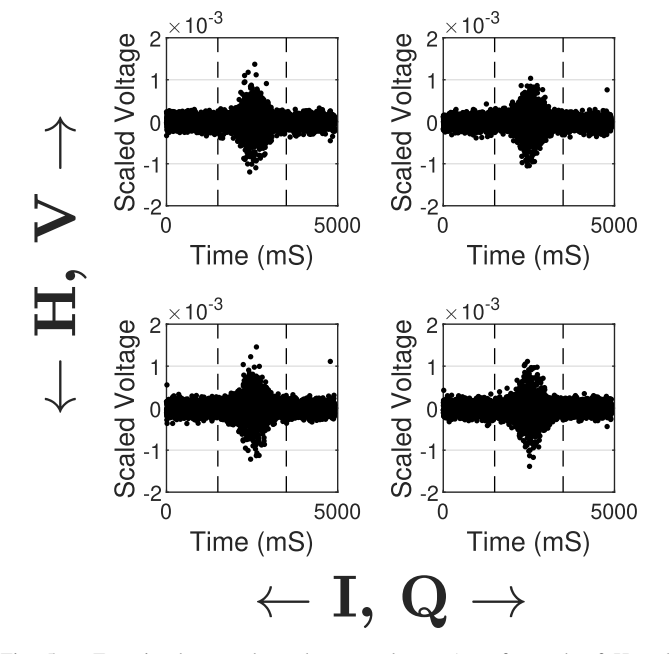


Fig. 5. Four in-phase and quadrature voltages (two for each of H and V polarizations), collected during a solar scan by the NCAR dual-polarized S-band radar, microsecond range samples recorded at millisecond intervals. The elevation for this data segment is held at 20.7° while the azimuth varies (4911 values along the horizontal axis). Voltages in A/D converter counts are given on the vertical axis (a.u. denoting arbitrary units). The broad hump in the middle is due to an alignment of the main S-Pol beam 0.92° wide with the sun, 0.53° wide. The dashed vertical lines indicate the hump portion that is removed in later plots. The data shown are for gate 1500, and the total number of gates is 1593, with the first 400 omitted in subsequent analysis.

sun (angular size 0.53°). Therefore, the zero-mean in-phase and quadrature time series are not statistically stationary in variance. To examine thermal noise (radar pointing at the sky)

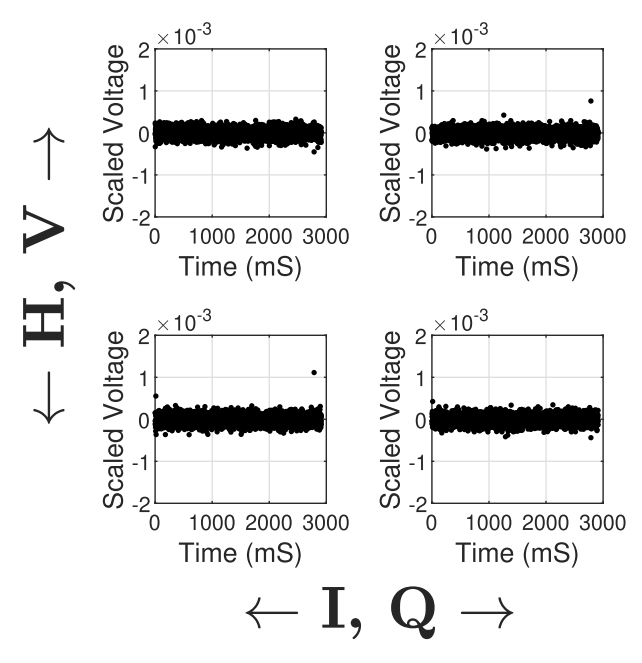


Fig. 6. As shown in Fig. 5 but with hump removed (times 1500–3500) so that the remaining N=2912 data points constitute stationary time series, aside from a couple of outliers (see below). The standard deviations are $\sigma_{\rm IV}=0.102\times 10^{-3}$, $\sigma_{\rm QV}=0.106\times 10^{-3}$, $\sigma_{\rm IH}=0.107\times 10^{-3}$, and $\sigma_{\rm QH}=0.104\times 10^{-3}$. The sample mean σ for the four plots is 0.105×10^{-3} , and all four standard deviations lie within 2σ of this value, where $\sigma=0.105\times 10^{-3}/(N)^{1/2}$ is an estimate of the standard error of the standard deviation. This is in accordance with sampling from the MCGM joint pdf (see main text).

parts of the data, we removed the solar hump as indicated by dashed vertical lines. The remaining data are shown in Fig. 6 and are wide-sense stationary [17] and zero-mean traces. This is important as the notion of the cross-correlation coefficient, strictly speaking, holds only for stationary time series, a point often forgotten in the literature, e.g., when examining weather echo signals. For example, ensuring orthogonality of the in-phase and quadrature components (sin and cos) at the chip level of an A/D converter does not render the resulting time series immune to spurious correlation due to nonstationary features such as the solar hump.

To test the remaining noise further for multivariate Gaussian characteristics (important, among other things, for the uniformity on the PS), the cumulative distribution is examined in Fig. 7 and the ACF is shown in the inset. The ACF is that of white noise, within sampling variability, considering that neither thermal noise nor solar microwave emission are coherent at a microsecond scale. A good agreement of the four data curves with the Gaussian cdf is seen (despite containing a couple of outliers) and the voltages, indeed, consist of independent samples drawn from a multivariate jointly normal circular distribution (MCGM, perhaps better recognized as the Rayleigh amplitude and uniform phase pdfs for each for the two polarizations).

Insofar as the multivariate Gaussian tests are single-point statistics, they are often blind to more subtle effects of nonstationarity, affecting two-point characteristics such cross correlation coefficients. Just a couple of outliers do not affect the former (based on population mostly) but do the latter.

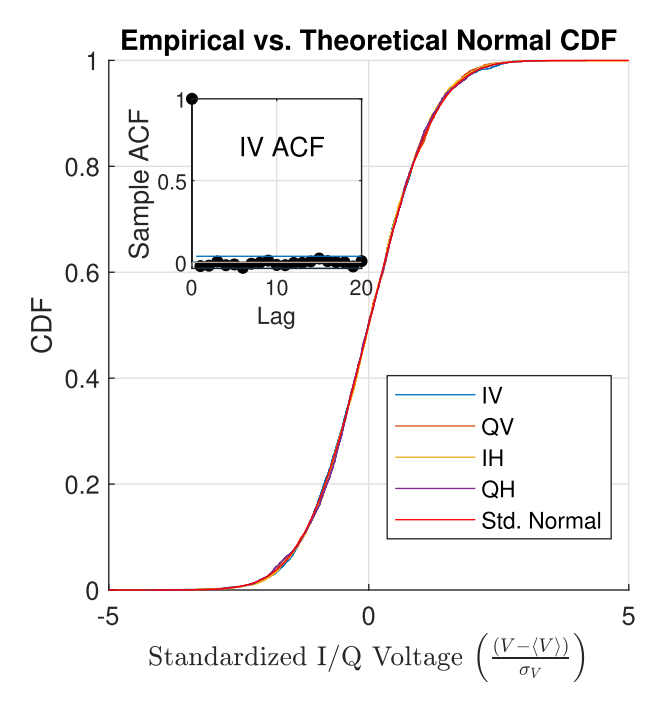


Fig. 7. Cumulative distribution function of the "humpless" data is close to a normal distribution. The four empirical distributions $(H/V \times I/Q)$ are plotted, as well as the standard normal distribution. All these appear to overlap at the resolution shown, despite including the outliers.

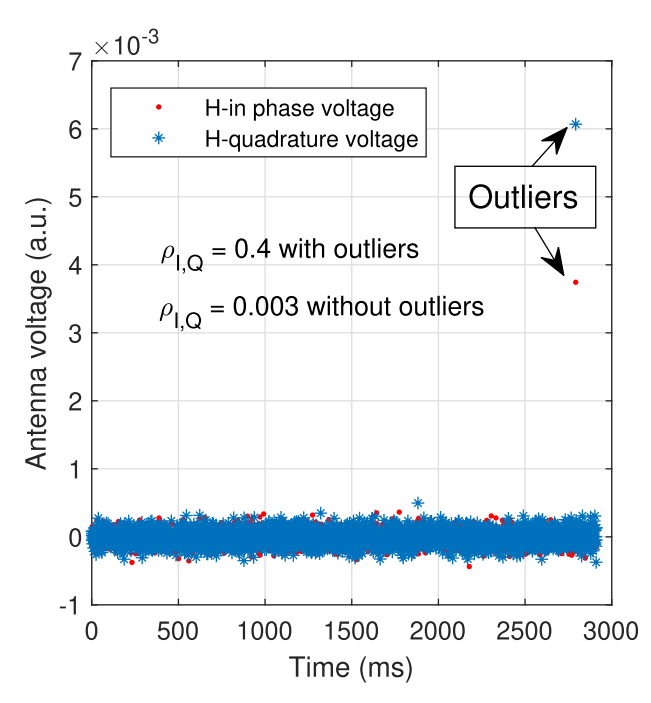


Fig. 8. Statistical stationarity versus orthogonality of I and Q components. Time-series for S-Pol H channel and gate 423, including extreme outliers at the far right, probably caused by a small plane or a flock of birds within S-Pol's beam. The two outliers here are at 42 σ and 68 σ (σ is the standard deviation of the time-series data). Upon removing the two outliers, $\rho_{\rm IQ}$ falls 0 within sampling variability, in accordance with I and Q orthogonality. Specifically, with the outliers, $\rho_{\rm IQ} = 0.4$ and without the outliers it is $\rho_{\rm IQ} = 0.003$, the latter well below the expected $1(N)^{-1/2}$ sampling variability of 0.02.

To that end, in Fig. 8, we examine the effect of outliers where one can see that although infrequent, these outliers affect the correlation coefficient a great deal. We used a generous threshold of 10σ to remove such outliers from

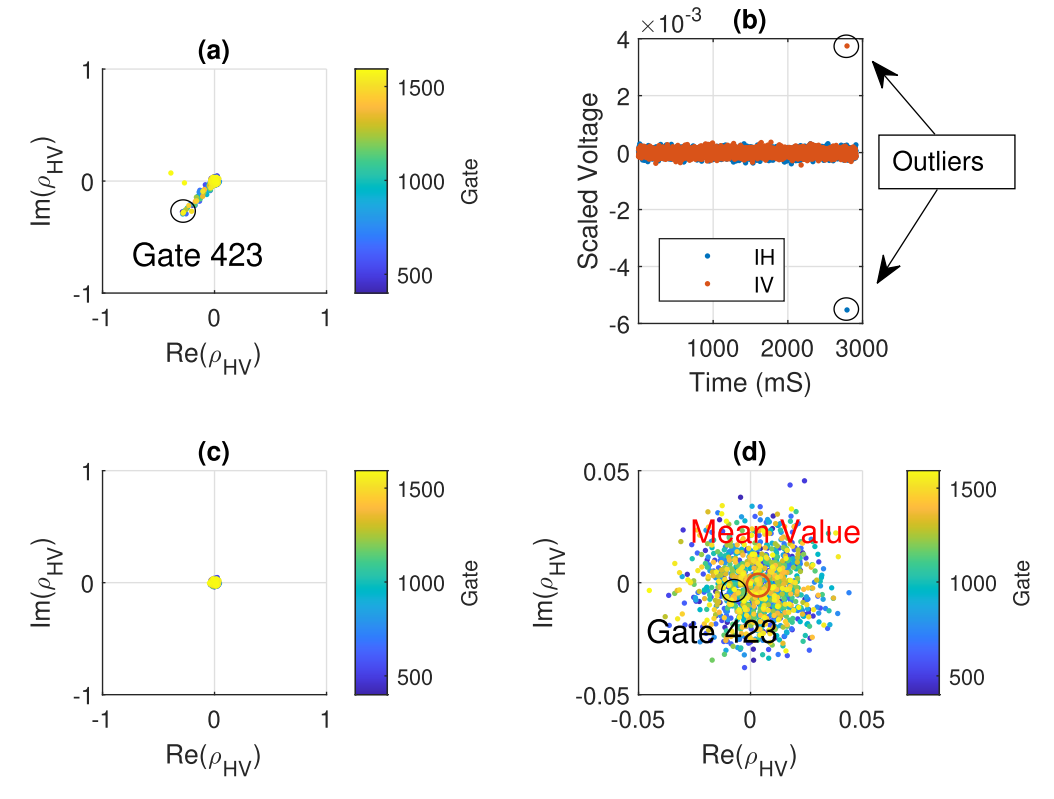


Fig. 9. S-Pol thermal noise data. (a) To avoid ground clutter, gates beyond 400 were used to calculate ρ_{HV} . An example gate with spuriously large ρ_{HV} is 423 (the tiny dot at the center of the black circle). (b) Time series associated with large value of ρ_{HV} in gate 423, showing outliers. (c) Values of ρ_{HV} for the same gates as in (a) but with the outliers removed; the threshold for outliers is about 10^{-3} or 10σ . (d) Closeup of (c). Bullseye coordinates (center of red circle): $\rho_{HV} = 0.003-0.001i$ and $\delta_{\tau} + i\delta_{\epsilon} = \text{Re}(\rho_{HV}) + i\text{Im}(\rho_{HV})$ yields the systematic tilt mismatch of $\delta_{\tau} = 0.17^{\circ}$ and $\delta_{\epsilon} = 0$ within sampling variability. Possible causes of the outliers include sidelobes seeing the sun, birds, or radio interference.

all-time series (gates) used and confirmed that there was no discernible change in the results when 5σ threshold was used.

Next, we get to the punchline and estimate polarization purity by estimating α via ρ by calculating the complex voltage cross-correlation coefficient ρ_{HV} as follows (see [11]):

$$\rho_{\text{HV}} = \frac{\sum_{i=1}^{N} V_{\text{H},i} V_{\text{V},i}^{*}}{\sqrt{\sum_{i=1}^{N} V_{\text{H},i} V_{\text{H},i}^{*} \sum_{i=1}^{N} V_{\text{V},i} V_{\text{V},i}^{*}}}$$
(20)

with the results displayed in the four panels (for many gates, one gate point on a plot) Fig. 9. It is seen from Fig. 9(a) of the figure that the values of ρ_{HV} are surprisingly large and follow a peculiar pattern, indicating nonstationary behavior, despite the solar hump removal. A common feature of those gates with large coefficients once again turns out to be the presence of rare but extreme outliers in the time-series as illustrated in Fig. 9(b). Once these outliers were removed with the simple 10σ threshold, a much closer clustering of coefficients about zero resulted as shown in (c) and the closeup in (d) of Fig. 9. Fig. 9(d) is the culmination of the analysis as the bullseye coordinates set bounds on polarization purity. As a reminder, to get to the bullseye, we avoided near gates, removed the hump, and filtered out extreme outliers.

While the sampling variability of an individual time series $\rho_{\rm HV}$ is about 0.02, that for bullseye coordinates is much more accurate as it is average over ≈ 1100 time series and there is an additional gain in accuracy of $1/(1100)^{1/2}$, or factor of 33. Thus, the bullseye coordinates are statistically accurate

to within $0.6 \times 10^{-3} = 1/1650$. This number is comparable to S-Pol cross-channel isolation of 2000 (Eric Loew, private communication).

Using $\delta_{\tau} + i\delta_{\epsilon} = Re(\rho_{\rm HV}) + i{\rm Im}(\rho_{\rm HV})$ and reading the RHS of the bullseye coordinates (red circle) in Fig. 9(d) yields the following bounds on the tilt and ellipticity mismatches: $\delta_{\tau} = 0.17^{\circ}$ and $\delta_{\epsilon} = 0.06^{\circ}$. The systematic ellipticity error is barely beyond sampling variability and should be regarded as statistically perfect (zero). This seems reasonable as the S-Pol polarization basis is linear and phase delays are not needed (in contrast to, say, circular polarization basis [34] or the slant 45° technique for generating HV basis, currently considered for phased array weather system and requiring a Φ phase shift. The S-Pol tilt mismatch is also remarkably low and does not get in the way of measuring such meteorological parameters as $Z_{\rm DR}$ and LDR. This method can be applied broadly, e.g., recent findings on polarization purity in borehole antennae [35].

VII. CONCLUDING REMARKS

In summary, our metric for the deviation from the basis orthogonality, α as defined by (2), can be regarded as a measure of polarization purity, designed to work with any polarization basis, not only the linearly polarized basis, discussed here or a circularly polarized basis. In that regard, this is a forward-looking approach, anticipating full polarimetric capability coming with the new generation phased array-based weather radars. Indeed, while phased array radars have a long

history, polarimetry with distributed sources of radiation is still relatively new. Possible dispersion in time and phase errors in these future systems with fully digital capability and potential to generate arbitrary polarization ellipses quickly as evolving basis states may benefit from our method. Cross coupling away from boresight and the biases can be estimated by the proposed framework as well. The analysis described here also suggests that examination of IQ traces via simple thresholding is quite efficient at detecting spurious outliers and benefits testing for Rayleigh-type statistics (MCGM), the ubiquity of which in weather signals is still an open problem.

The S-Pol test results are encouraging as the α approach leads to polarization purity estimates close to the S-Pol polarization isolation factor of 2000 (Eric Loew, private communication) as well as other metrics of polarization purity. The S-Pol radar uses a Potter feed to illuminate the parabolic reflector dish. The Potter feed offers broadband performance and beam symmetry for a linear dual-polarimetric radar configuration. Unbiased estimation of co- and cross-pol measurements depends on matching and orthogonality in polarization basis between horizontal and vertical co-polarizations and having a minimum of cross-pol response at the co-pol radiation pattern maximum. In addition to the above-mentioned requirements of antenna illumination feed, surface smoothness of the parabolic reflector better than 0.1 of transmit wavelength is required to minimize crosstalk between co- and cross-polarization signals and minimize bias in depolarization measurements due to the radar system.

Our main result is (18) and its derivation relies on two layers of orthogonality: the geometric (polarization states) and the stochastic (random variables). The latter stems from the fact that a cross-correlation coefficient can be viewed as a cosine of an angle between two random variables regarded as elements of an abstract vector space because an expectation value of a product of two random variables satisfies all properties of an inner product [17]. In this purely mathematical sense, our results may be unique insofar as they relate abstract angles in a functional space with concrete tangible angles in real 3-D space of polarized waves.

The derivation also requires sufficient randomness of polarimetric noise so that probability has a simple measure such as area on the PS. We expect that the uniformity on the sphere requirement can be softened, e.g., replaced by the symmetry with respect with the antenna basis at hand. If so, precipitation itself may supply "calibration noise" and work in this direction is ongoing. During precipitation observations (rather than thermal noise), *N* is a number of correlated (rather than independent) samples but one considers whitening the data to reduce the correlation [36]. For non-Gaussian radiation, one that is nonuniformly distributed on the PS, or general and otherwise unrestricted IID radiation, the numerical prefactors such as in (15) can be derived in a similar manner and would, generally, differ from unity.

Finally, it has not escaped our attention that the technique proposed here is generic and, in addition to already mentioned polarimetric weather radars operating in a circular basis [34], can be applied to any antenna system capable of generating circular or elliptical polarization whether phased array-based

or not, particularly in the area of wireless communications [37] and biomedical devices [38]. This work focused on estimating polarization purity of receivers but transmitters can also be tested by measuring α , e.g., in bistatic cases, transmitter in question can send polarized waves directly to a previously calibrated receiver or use "mirror-like" targets.

ACKNOWLEDGMENT

Alexander Kostinski is grateful to the University Corporation for Atmospheric Research Affiliate Scientist Program for their support. The authors are grateful to John Hubbert, Eric Loew, Michael Dixon, and Ulrike Romatschke for helpful comments regarding National Center for Atmospheric Research (NCAR), S-Pol radar data.

REFERENCES

- R. Rotman, M. Tur, and L. Yaron, "True time delay in phased arrays," Proc. IEEE, vol. 104, no. 3, pp. 504–518, Mar. 2016.
- [2] R. D. Palmer et al., "Horus—A fully digital polarimetric phased array radar for next-generation weather observations," *IEEE Trans. Radar* Syst., vol. 1, pp. 96–117, 2023.
- [3] D. S. Zrnic, G. Zhang, and R. J. Doviak, "Bias correction and Doppler measurement for polarimetric phased-array radar," *IEEE Trans. Geosci. Remote Sens.*, vol. 49, no. 2, pp. 843–853, Feb. 2011.
- [4] G. Zhang, R. J. Doviak, D. S. Zrnić, R. Palmer, L. Lei, and Y. Al-Rashid, "Polarimetric phased-array radar for weather measurement: A planar or cylindrical configuration?" *J. Atmos. Ocean. Technol.*, vol. 28, no. 1, pp. 63–73, Jan. 2011.
- [5] Z. Wang and A. B. Kostinski, "A random wave method for detecting phase imbalance in a coherent radar receiver," *J. Atmos. Ocean. Technol.*, vol. 10, no. 6, pp. 887–891, Dec. 1993.
- [6] B. H. Suits, A. B. Kostinski, and M. D. Kulkarni, "Monitoring quadrature phase error and gain mismatch using noise," *J. Magn. Reson., Ser. A*, vol. 108, no. 2, pp. 230–233, Jun. 1994.
- [7] M. D. Kulkarni and A. B. Kostinski, "A simple formula for monitoring quadrature phase error with arbitrary signals," *IEEE Trans. Geosci. Remote Sens.*, vol. 33, no. 3, pp. 799–802, May 1995.
- [8] J. W. Goodman, Statistical Optics. Hoboken, NJ, USA: Wiley, 1985.
- [9] V. N. Bringi and V. Chandrasekar, *Polarimetric Doppler Weather Radar:* Principles and Applications. Cambridge, U.K.: Cambridge Univ. Press, 2001.
- [10] M. Sachidananda and D. S. Zrnic, "ZDR measurement considerations for a fast scan capability radar," *Radio Sci.*, vol. 20, no. 4, pp. 907–922, Jul. 1985.
- [11] J. C. Hubbert, S. M. Ellis, M. Dixon, and G. Meymaris, "Modeling, error analysis, and evaluation of dual-polarization variables obtained from simultaneous horizontal and vertical polarization transmit radar. Part I: Modeling and antenna errors," *J. Atmos. Ocean. Technol.*, vol. 27, no. 10, pp. 1583–1598, Oct. 2010.
- [12] A. Kostinski and W. Boerner, "On foundations of radar polarimetry," IEEE Trans. Antennas Propag., vol. AP-34, no. 12, pp. 1395–1404, Dec. 1986.
- [13] M. Born and E. Wolf, Principles of Optics. Oxford, U.K.: Pergamon Press, 1983.
- [14] C. Brosseau, Fundamentals of Polarized Light: A Statistical Optics Approach. Hoboken, NJ, USA: Wiley, 1998.
- [15] B. Yen Toh, R. Cahill, and V. F. Fusco, "Understanding and measuring circular polarization," *IEEE Trans. Educ.*, vol. 46, no. 3, pp. 313–318, Aug. 2003.
- [16] G. Zhang, Weather Radar Polarimetry. Boca Raton, FL, USA: CRC Press, 2016.
- [17] A. Papoulis and S. U. Pillai, Probability, Random Variables and Stochastic Processes. New York, NY, USA: McGraw-Hill, 2002.
- [18] R. J. Doviak, Doppler Radar and Weather Observations. Chelmsford, MA, USA: Courier Corporation, 2006.
- [19] A. B. Kostinski, "Fluctuations of differential phase and radar measurements of precipitation," *J. Appl. Meteorol.*, vol. 33, no. 10, pp. 1176–1181, Oct. 1994.

- [20] J. Vivekanandan and E. Loew, "Airborne polarimetric Doppler weather radar: trade-offs between various engineering specifications," *Geoscientific Instrum.*, *Methods Data Syst.*, vol. 7, no. 1, pp. 21–37, Jan. 2018.
- [21] G. Zhang, R. J. Doviak, D. S. Zrnic, J. Crain, D. Staiman, and Y. Al-Rashid, "Phased array radar polarimetry for weather sensing: A theoretical formulation for bias corrections," *IEEE Trans. Geosci. Remote Sens.*, vol. 47, no. 11, pp. 3679–3689, Nov. 2009.
- [22] E. Loew and J. Vivekanandan, "An investigation of the requirements of an airborne, scanning, polarimetric phased array radar to accurately measure hydrometeor properties near the earth's surface," in *Proc. 38th Conf. Radar Meteorol.*, 2017, p. 1.
- [23] J. W. Goodman, Speckle Phenomena in Optics: Theory and Applications. Greenwood Village, CO, USA: Roberts and Company Publishers, 2007.
- [24] G. Sinclair, "The transmission and reception of elliptically polarized waves," *Proc. IRE*, vol. 38, no. 2, pp. 148–151, Feb. 1950.
- [25] R. E. Collin, Antennas and Radiowave Propagation. New York, NY, USA: McGraw-Hill, 1985.
- [26] A. R. Jameson and S. L. Durden, "A possible origin of linear depolarization observed at vertical incidence in rain," *J. Appl. Meteorol.*, vol. 35, no. 2, pp. 271–277, Feb. 1996.
- [27] A. B. Kostinski, B. D. James, and W.-M. Boerner, "Optimal reception of partially polarized waves," *J. Opt. Soc. Amer. A, Opt. Image Sci.*, vol. 5, no. 1, p. 58, Jan. 1988.
- [28] D. Kestner and A. Kostinski, "Simple formula for the Jones product and the pancharatnam connection in optics," *Phys. Rev. A, Gen. Phys.*, vol. 109, no. 2, Feb. 2024, Art. no. 023517.
- [29] D. Kestner, "Applications of independent and identically distributed (IID) random processes in polarimetry and climatology," Ph.D. dissertation, Dept. Phys., Michigan Technol. Univ., Houghton, MI, USA, 2023.
- [30] J. Ellis and A. Dogariu, "Differentiation of globally unpolarized complex random fields," J. Opt. Soc. Amer. A, Opt. Image Sci., vol. 21, no. 6, p. 988, Jun. 2004.
- [31] N. Fisher, T. Lewis, and B. Embleton, Statistical Analysis of Spherical Data. Cambridge, U.K.: Cambridge Univ. Press, 1987.
- [32] J. C. Hubbert, J. W. Wilson, T. M. Weckwerth, S. M. Ellis, M. Dixon, and E. Loew, "S-Pol's polarimetric data reveal detailed storm features (and insect Behavior)," *Bull. Amer. Meteorolog. Soc.*, vol. 99, no. 10, pp. 2045–2060, Oct. 2018.
- [33] PRECIP NCAR S-Pol Radar Time Series Data. Version 1.0. UCAR NCAR Earth Observing Laboratory, document NCAR/EOL S-Pol Team, 2023, doi: 10.26023/EMAT-JPBX-S20T.
- [34] G. C. McCormick and A. Hendry, "Principles for the radar determination of the polarization properties of precipitation," *Radio Sci.*, vol. 10, no. 4, pp. 421–434, Apr. 1975.
- [35] S. Ebihara, K. Toyozawa, T. Hasegawa, Y. Tsujikawa, and K. Koyama, "Influence of a horizontally polarized wave incidence on DOA estimation by a dipole array antenna in a borehole," *IEEE Trans. Geosci. Remote Sens.*, vol. 62, 2024, Art. no. 1000116.
- [36] A. C. Koivunen and A. B. Kostinski, "The feasibility of data whitening to improve performance of weather radar," *J. Appl. Meteorol.*, vol. 38, no. 6, pp. 741–749, 1999.
- [37] I. Nadeem et al., "A comprehensive survey on 'circular polarized antennas' for existing and emerging wireless communication technologies," J. Phys. D, Appl. Phys., vol. 55, no. 3, Jan. 2022, Art. no. 033002.

[38] M. E. Yassin, K. F. A. Hussein, Q. H. Abbasi, M. A. Imran, and S. A. Mohassieb, "Flexible antenna with circular/linear polarization for wideband biomedical wireless communication," *Sensors*, vol. 23, no. 12, p. 5608, Jun. 2023.



Alexander Kostinski has been with Michigan Technological University since 1989, where he is a Professor of Physics. He has been funded by the National Science Foundation for over 30 years as a sole PI and his publications have ranged broadly from optics, fluid mechanics and astrophysics to radar meteorology, atmospheric science and statistical signal analysis. He has taught most of the graduate and senior bachelor's courses offered by the MTU Physics Department. He is currently contributing to the APAR program. He is also currently

an Affiliate Scientist at the National Center for Atmospheric Research.



Daniel Kestner received the B.Sc. degree from Michigan Technological University, Houghton, MI, USA, in 2009, and the M.S. degree from Ohio State University, Columbus, OH, USA, in 2013. He is currently finishing up the Ph.D. degree with the Department of Physics, Michigan Technological University.

His research interests include optical and radar polarimetry, meteorology, statistical signal analysis, and data science.



Jothiram Vivekanandan is a Senior Scientist at Earth Observing Laboratory, NCAR, Boulder, Colorado, USA. His research and development breadth includes polarimetric radar, dual-wavelength radar, phased array radar, lidar, and microwave radiometer. Prime examples of his leadership are his development of a dual-wavelength radar system, created by adding a millimeter-wave radar to the NCAR's S-band polarization radar (S-Pol), and his scientific and technical leadership to the development of an NSF-funded cloud radar for Gulf Stream

V research aircraft. He led the composition of the NSF MSRI-2 Airborne Phased Array Radar (APAR) proposal Project Description (PD), working closely with the APAR team. The PD made a compelling case for the need for APAR and NSF funded the \$90M APAR project. He is the APAR science and engineering liaison. APAR is a dual-Doppler and dual-polarimetric weather radar system on C-130 aircraft, which will enable more accurate weather forecasting. It is a transformative technology for weather remote sensing with several novel ideas and concepts.

Dr. Vivekanandan is a Fellow of the American Meteorological Society and an Associate Editor for Radio Science. The 2018 European Geophysical Union's Christiaan Huygens Medal was awarded for his pioneering and ground-breaking work on the microphysical characterization of clouds and precipitation using advanced remote sensors.